HYDROSTATIC BULGING OF ELIPTICAL SINGLE AND LAMENATED SHEET METALS

Salem A. Ammar, N.R Chitkara* and Ramadan O. Saied

Mechanical Department, Faculty of Engineering, University of Tripoli
*Applied Mechanics Division, Mechanical Department, UMIST, UK
E-mail: saied972004@yahoo.com,

الملخص

يقدم هذا البحث دراسة اختباريه ونظرية علي الانتفاخ الهيدروليكي للرق الأهليلجي (قطاع ناقص) المفرد والمزدوج والمصنوع من معدن الحديد المطاوع ومن معدن الألمونيوم. أجريت اختبارات الانتفاخ على المعدنين باستخدام جهاز ضغط هيدروليكي يعمل بضغط الزيت ومركب عليه قالب اهليجي (قطاع ناقص) لغرض تحديد الخواص الميكانيكية للصفائح المستخدمة ومعرفة أنماط التكسر وأجريت تجارب الشد علي بعض العينات من الحديد والألمونيوم. كما تم قياس ضغوط الانتفاخ والانفعالات الطولية والمستعرضة والسمكية للعينات بعد تشكلها معمليا وتم حسابها نظريا. من خلال التجارب استنتج أن العينات المصنوعة من الحديد اكتسبت ضغط انتفاخي أعلى من العينات المصنوعة من الألمونيوم وأن آلية تحطم الرق المفرد للألمونيوم والحديد يكون عن طريق حدوث شق في منطقة التاج أو عند الحافة.

ABSTRACT

This paper presents an experimental and theoretical study on the hydrostatic bulging of single and laminated elliptical sheets (diaphragms) made of aluminum and mild steel materials. The bulge tests were carried out on the sheets at rolling direction parallel and transverse to the major axes of the diaphragms. Furthermore, the sheets were tested one over the another and vice versa. Theoretical expressions were developed to predicate the bulge pressure and strains of diaphragms. In order to determine the yielding stresses of the materials, tensile tests were carried out on samples from mild steel and aluminum materials. A method for measuring the experimental strains along the minor and major axes of bulge diaphragms was developed. Detailed observations were made on the characteristic modes of failure of tested diaphragms. It was concluded that the maximum bulge pressure of single mild steel diaphragm was considerably more than in the case of aluminum diaphragm and the crackes of the single sheet or laminated diaphragms occurred either near the pole or at the edge of diaphragms.

KEYWORDS: Diaphragm; Bulge Bressure; Elliptic Die; Strains; Mild Steel; Aluminum.

INTRODUCTION

The increasing requirement of the sheet metals by industry has led to many studies being conducted to investigate sheet metal properties under simple and complex loading conditions. Testing of sheet metals under hydrostatic bulge loading is an interesting way to determine the flow stress-strain characteristics of the sheet metal. The important advantage of this test that there is no contact (friction) between specimens and tools in the region of bulging, which allows tosimplify the theatrical

analysis for stress- strain and increase test accuracy [1]. Furthermore, the bulge test can be used to determine the strain hardening, and plastic properties of sheet metals [2-4]. The hydraulic bulge test is interesting subject of many researches. Yousif et al [5] investigated the deformation and failure mechanisms of the rectangular diaphragms. They found that the diaphragm either ruptured along the edge or the pole along the major axis depending on the aspect ratio of the ellipse and diaphragm material. Tomov et al[6] outlined the mechanical conditions when sheet metals tested by hydraulic bulging. They found that the mechanical state of sheet bulging can be analyzed in more general way without any restrictions to the loading rate and pressure distributions.

Kim et al [7] used an aero-bulge test to characterise the plastic behavior of a very thin copper foils. They introduced an analytical model for calculating the dome radius and thickness at the crown area. Recently, Sobotka et al [8] introduced a new plasticity yield criterion (so called Vegter yield) by using the bulge test. This criterion accurately matches to the deformation behavior of highly anisotropic materials. More recently, Tonging et al [9] studied the surface effect on the mechanical behavior of the bulge membrane at nano-scale using combined continuum theories and atomistic simulations. Janbakhsh et al [10] performed bulge and uniaxial tests to determine the flow stress curves of four different sheet metal alloys and they reported that the hydrostatic bulge test provided flow stress properties at higher strain levels as compared to uniaxial loading.

Although considerable researches have been devoted to the behavior of single sheet under bulging pressure, rather less attention has been paid to laminated sheets [11-13]. Therefore, it is the purpose of the present paper to study experimentally and theoretically the deformation behavior and characteristic of the equivalent strains of single and laminated sheets of the mild steel and aluminum materials under hydrostatic bulge test.

EXPERIMENTAL WORK
Material

Materials used for experiments are mild steel sheets with thickness of 0.833 mm and deep drawn aluminum sheets with thickness of 0.66 mm. Table 1 shows the measured mechanical properties of two materials according to the SA370 standard method [14].

Table 1: Measured mechanical properties of aluminum and mild steel sheets

Material	σ_{yp} (MPa)	σ_{ut} (MPa)	ε_{yp} (%)	ε_{ut} (%)	E (MPa)
Mild steel	230	325	1.2	18	200
Aluminum	100	120	0.18	20	70

Preparation of the Specimens

Several specimens, for bulge tests, with dimension of 194x155mm, were cut as received condition without annealing from the two sheets at rolling direction parallel and transverse to the major axis. Each specimen was scribed lightly on one side in form lines of 5 x 5 mm square grid net work. These lines were used to measure the longitudinal and transverse strains of the bulged specimen.

The Bulge Test Rig

Figure (1a) shows a photograph of the test rig. It consists of an elliptical die, working table, high pressure hydraulic pump, pipe fittings, pressure transducers, pressure gauges and instrumentation connections. The die was machined from a hard steel plate with thickness 80 mm. The die consists of two main parts, the base plate and clamping plate that contained an aperture profile with required shape of diaphragm (see Figure 1b). Several holes were drilled in the base plate for hydraulic and measurement connections.
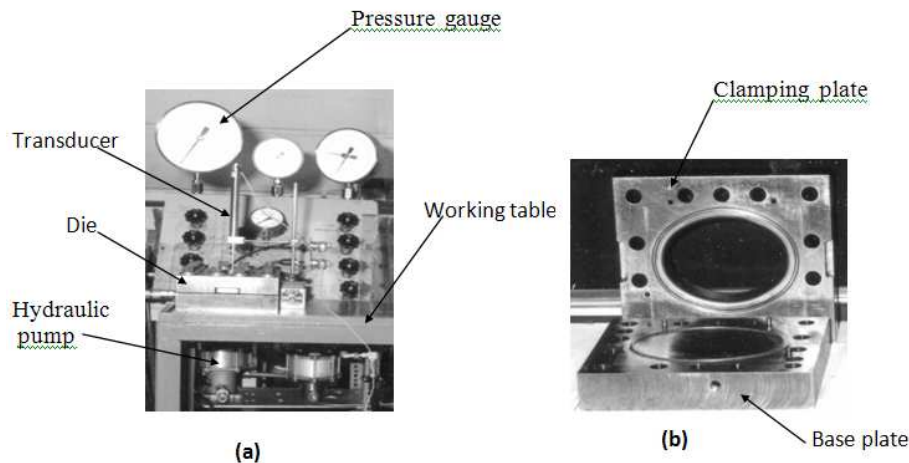

Figure 1: (a) test rig, (b) elliptic die

Bulge Test Procedure

The bulge test was carried out by placing a specimen between two parts of the die and then clamped together by high strength bolts. A hydrostatic pressure was applied on the specimen by the hydraulic pump until the bulge failure take place. The continuous data of pressure and displacement readings were sent to the computer through a data acquisition.

Strain Measurements

After finishing the test, displacements (x_{i+1}) and (y_i) were measuring by sticking a transparent stripe sheet (25x200mm) along the major and minor axes of deformed (bulged) sheet using sticky tape. This sticky tape allowed the deformed positions of nodal points marked previously on the sheet were then carefully marked onto the transparent strip using any sharp edged tool and then the displacement between deformed nodes were measured by vernier microscopic. The final thickness (t_i) of the bulged diaphragm at various points was measured by passing the deformed diaphragm between fixed ball and digital dial gauge. From these measurements, the longitudinal, transverse and thickness strains were calculated using the following equations:

$$\varepsilon_x = \ln[\frac{x_{i+1} - x_i}{5mm}] \tag{1}$$

$$\varepsilon_y = \ln[\frac{y_i}{5mm}] \tag{2}$$

$$\varepsilon_t = \ln\left[\frac{t_i}{t_o}\right] \tag{3}$$

where, $\varepsilon_x, \varepsilon_y$ and ε_t are the longitudinal, transverse and thickness strains respectively and 5 mm was the original distance between each grid. (x_{i+1}) and (x_i) are the final and initial longitudinal distances respectively.

THEORTICAL ANALYSIS
Plastic Deformation of Laminated Diaphragms

In order to develop the theoretical analysis of the plastic deformation of the elliptical laminated diaphragm, it was assumed that the sheets are initially elliptic in shape, clamped rigidly around their edges and subjected to uniform hydrostatic pressure on one side. Figure (2) shows a schematic view of a elliptical diaphragm deformed out of plane at a stage deformation where the laminated sheets are stacked together and remain in contact during the deformation. During the deformation of sheets, it was observed that the profile shapes for minor axis was closely circular whereas for major axis, the radius of curvature at the pole initially slightly less than and finally greater than at the edges and therefore, the profile shape may be approximated as circular.
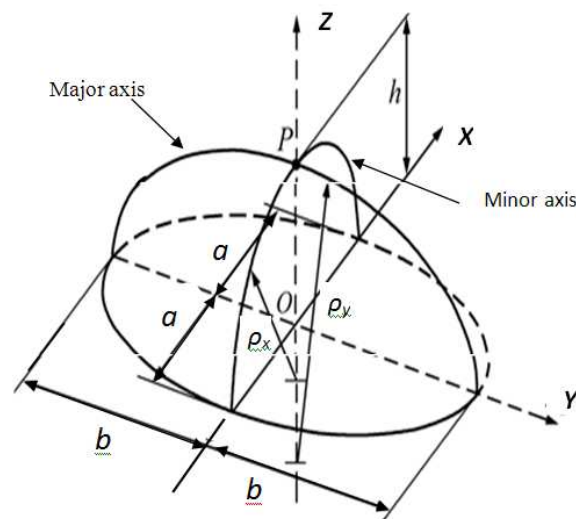

Figure 2: Schematic view of a elliptic diaphragm under bulging pressure [1]

Thus for deformed elliptical diaphragm shown schematically in Figure (2), the radii of curvatures of the minor (ρ_x) and major (ρ_y) axes are given by:

$$\rho_x = \frac{h^2 + a^2}{2h} \tag{4}$$

$$\rho_y = \frac{h^2 + b^2}{2h} \tag{5}$$

Strain on the Major Axis

The strain along the major axis was developed by assuming that the trajectory of a point on the major axis near the pole was orthogonal to the profile at any instant.

Figure (3) shows an element from the deformed diaphragm along the major axis with arc length of $\rho_y \, d\theta$ [5] .
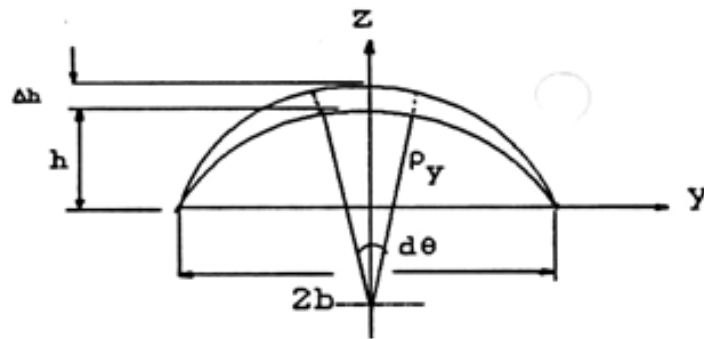

Figure 3: a view of an element from deformed diaphragm along the major axis [5]

When the pressure is increased by say dp, the height of the crown increases by dh. Therefore, the strain ($d\varepsilon_y$) on the element can be calculated as:

$$(d\varepsilon_y)_{y=0} = \frac{(\rho_y + dh)d\theta - \rho_y \, d\theta}{\rho_y \, d\theta} = \frac{dh}{\rho_y} \tag{6}$$

Substituting equation (5) in (6) and integrating, lead to the total strain at the pole along the major axis as:

$$(\varepsilon_y)_{y=0} = ln\left[\frac{h^2 + b^2}{b^2}\right] \tag{7}$$

Strain on the Minor Axis

By adopting a similar procedure, the longitudinal strain along the minor axis can by found as :

$$(d\varepsilon_x)_{x=0} = ln\left[\frac{h^2 + b^2}{a^2}\right] \tag{8}$$

Thickness Strain

The thickness strain can be deduced[5] as :

$$\varepsilon_t = -(\varepsilon_x + \varepsilon_y) \tag{9}$$

Thus :

$$\varepsilon_t = -\left(ln\left[\frac{h^2 + b^2}{a^2}\right] + ln\left[\frac{h^2 + b^2}{b^2}\right] \right) \tag{10}$$

The strain ratio at the pole where x = 0 and y = 0 is:

$$\frac{\varepsilon_x}{\varepsilon_y} = \frac{ln\left[\frac{h^2 + b^2}{a^2}\right]}{ln\left[\frac{h^2 + b^2}{b^2}\right]} \tag{11}$$

Equilibrium Equation

The equilibrium equation for a laminated sheet, for example mild steel and aluminum sheets, at the pole may be derived by considering the stress distribution on a small elemental strip (see Figure 4) of deformed laminated sheet of current thickness t_s

and t_a for the steel and aluminum respectively while the total thickness is t_t when the laminated sheet is deformed under the pressure P.
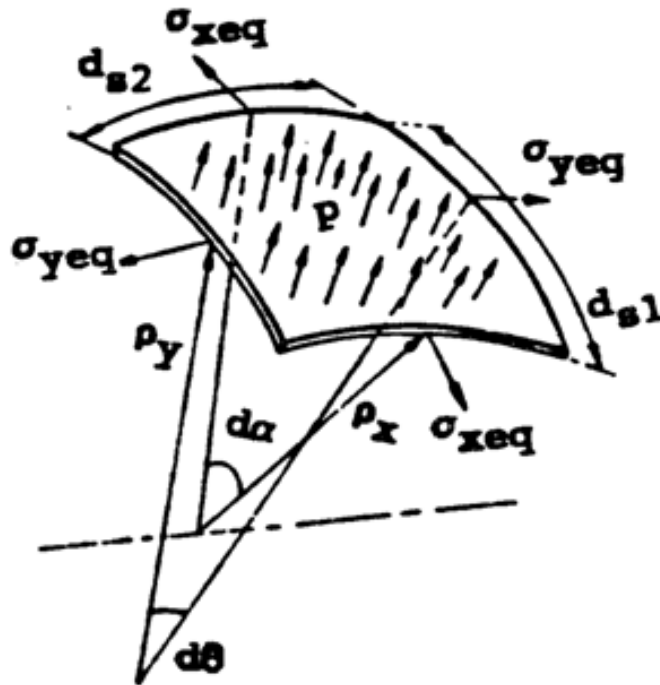

Figure 4: Schematic a view of element at the pole of bulging diaphragm [5]

The forces acting on the element in radial direction, leads to the following equilibrium equation [12]:

$$P = t_t \left[\frac{\sigma_{xeg}}{\rho_x} + \frac{\sigma_{yeg}}{\rho_y} \right] \qquad (12)$$

and

$$\sigma_{xeg} = \frac{(\sigma_{xs} t_s + \sigma_{xa} t_a)}{(t_s + t_a)} \qquad , \qquad \sigma_{yeg} = \frac{(\sigma_{ys} t_s + \sigma_{ya} t_a)}{(t_s + t_a)} \qquad (13)$$

RESULTS AND DISCUSIONS

Tables (2a and 2b) show the effect of the rolling direction on the failure pressure of the single and laminated sheets. It can be observed that there is no effect of rolling direction on the single sheet of mild steel and laminated sheet of steel on aluminum. However, there is a slightly effect on the single aluminum and laminated sheet of aluminum on steel. The significant increase of bulge pressure can be observed between the single bulging sheet and the laminated sheets.

Table 2a: Failure pressure of sheets with rolling direction parallel to major axis

| Description	Single sheet mild steel	Single sheet Aluminum	Laminated sheet Aluminum on steel	Laminated sheet Steel on Aluminum
Failure pressure	7.5 MPa	0.83 MPa	9.1 MPa	9.2 MPa

Table 2b: Failure pressure of sheets with rolling direction transverse to major axis

Description	Single sheet mild steel	Single sheet Aluminum	Laminated sheet Aluminum on steel	Laminated sheet Steel on Aluminum
Failure pressure	7.5 MPa	1.08 MPa	9.4 MPa	9.2 MPa

Figure (5a) shows the pressure - deflection curves for bulged laminated diaphragms (aluminum staked on mild steel and vise verse) with rolling direction transverse to the major axis. It can be seen that at early stages of bulging, the both laminates exhibited same bulging pressure up to the deflection of 10 mm and then the pressure of laminated (mild steel staked on aluminum) became higher up to the deflection of 35 mm. Figure (5b) shows the comparison between the theoretical and experimental of pressure-deflection curves of the laminated diaphragm (aluminum staked on mild steel). The two curves are compared well up to the deflection of 16 mm and then they diverged in which the experimental pressure increased by approximately 25% than the theoretical one. This is probably due to the strain hardening effect. All the curves of tested diaphragms exhibited the same behavior and showed nonlinearity which probably due to the ductility (plasticity) of the materials which allowed to high plastic deformation occurs at high strain rate.
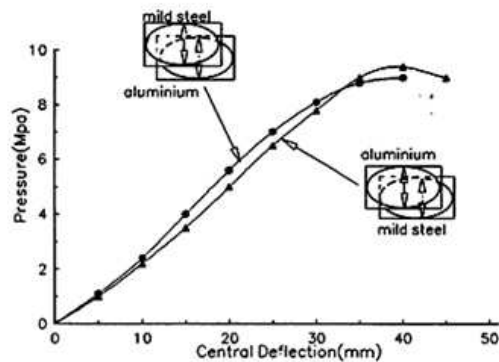
(a)
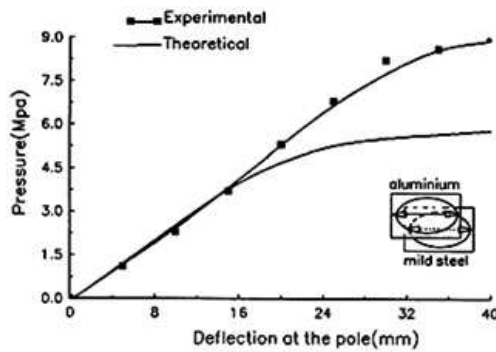
(b)

Figures 5 (a and b) : Pressure-deflection curves for laminated diaphragms

Fracture Modes

Figure (6a and 6b) shows photographs of fracture modes of mild steel sheet with rolling direction parallel and transverse to the major axes respectively. It can be seen that the bulge shape of two sheets along the two axes are almost circle. This observation was a adopted in the above theoretical analysis. The fracture appeared as small tear almost near the pole and in direction along the major axis. This fracture mode is similar to that reported by Gutscher et al [16] in their study.
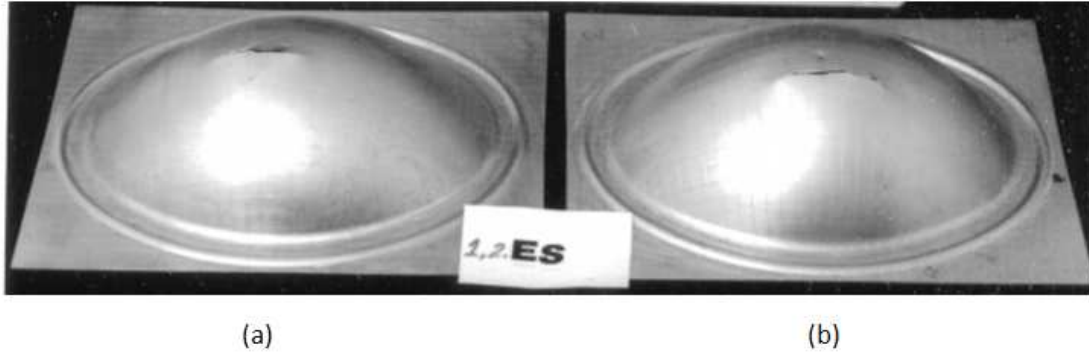

(a)   (b)

Figure 6: Modes of fracture of mild steel sheets with rolling direction, (a) Parallel to major axis, (b) transverse to major axis

Figure 7 (a and b) shows the modes of fracture of laminated sheet of mild steel staked on aluminum and tested with rolling direction parallel to the major axis. The mild steel diaphragm was punched near to the pole where as fracture of the aluminum diaphragm spared around the circumferential at the clamped edge, which probably due to the effect of friction and stress concentration at the edges.
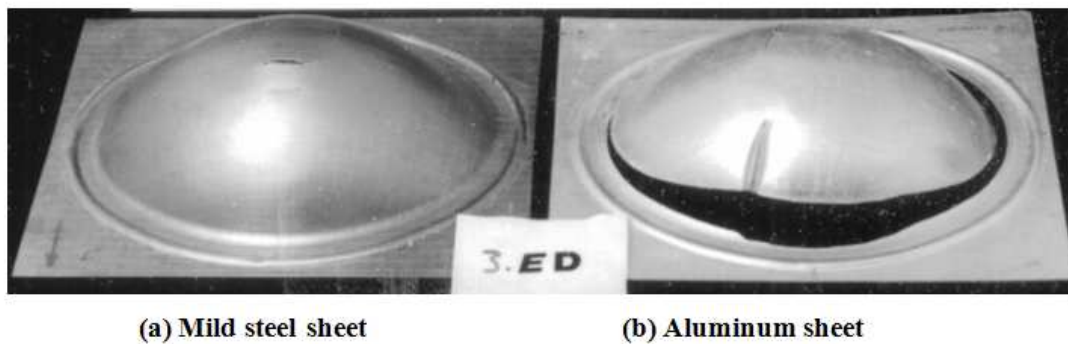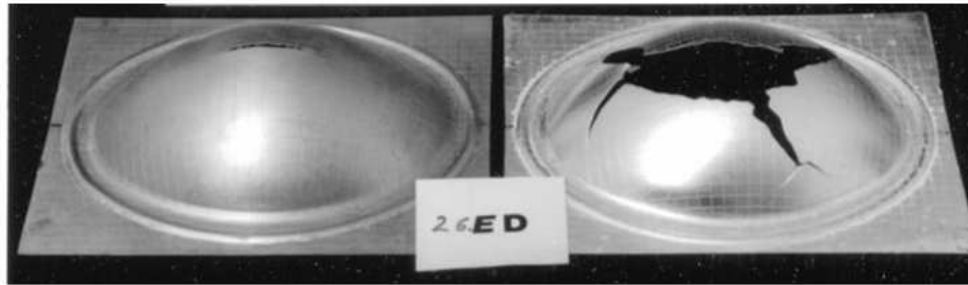

(a) Mild steel sheet   (b) Aluminum sheet

Figure 7: Modes of fracture of laminated sheet of mild steel (a), stacked on the aluminum sheet (b), with rolling direction Parallel to major axis

Figure (8a and 8b) shows mode of fracture of a laminated sheet of aluminum stacked on the mild steel and tested with rolling direction parallel to the major axis. Compare with the deformation mode in Figure (4), it can notes that the aluminum diaphragm(Figure 8b) fractured by burst at the pole due to the high bulged pressure which was produced by the small crack at the crown of the mild steel diaphragm under net of aluminum diaphragm.

(a) Mild steel sheet   (b) Aluminum sheet

Figure 8: Modes of fracture of laminated sheet of aluminum sheet (b) , stacked on the mild steel sheet (a), with rolling direction Parallel to major axis

Strain Distributions along the Minor Axis

Figure (9a and 9b) shows the longitudinal (ε_x), transverse (ε_y) and thickness (ε_t) strains versus the distance from the pole along the minor axis for (a) mild steel single sheet and for (b) laminated sheet (Mild steel stacked on aluminum sheet). It can be seen that the experimental and theoretical of strains exhibited their maximum values near the pole and then decreased gradually toward the clamped edge. The thickness strains (ε_t) in both figures became constant for a short distance near the edge, while (ε_x), (ε_y) values drop continuously, in which the values of longitudinal strain (ε_y) are much lower and almost zero at the edge. The dotted line of the experimental curves near the pole indicted that there is an area near the pole where, the values of (ε_x), (ε_y) and (ε_t) could not be measured accurately because of failure of the diaphragm. The characteristic of the theoretical strain curves are linear and the experimental values distributed around it. The correlation between theoretical and experimental strains is reasonable satisfactory.
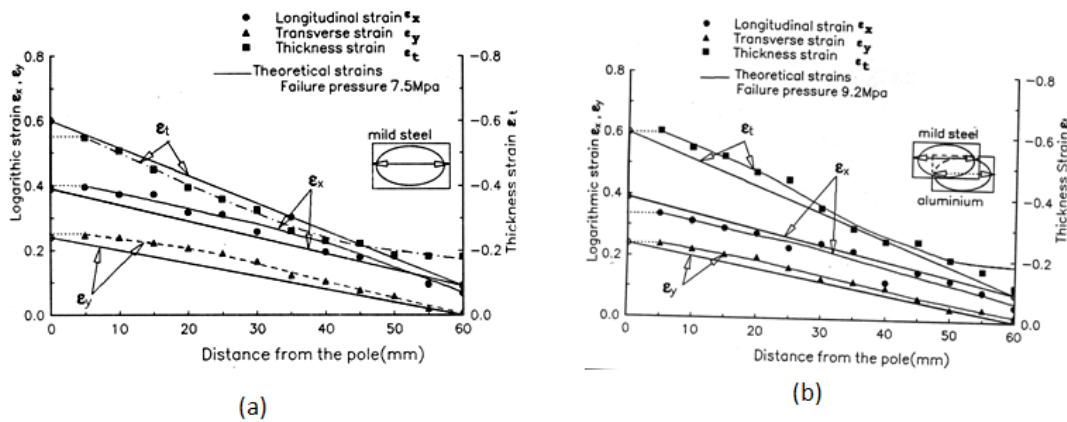

Figure 9: Strain distribution along the minor axis (a) single mild steel diaphragm, (b) laminated mild steel stacked on aluminum diaphragm. The dotted lines (…..) means that the strain at the region unmeasured due because of failure of the diaphragm.

CONCLUSIONS

Based on the above investigations, a number of conclusions were drawn as follows:

- The maximum bulging pressure of single mild steel diaphragm was considerably higher than in the case of aluminum diaphragm.
- No significant increase in resistance was offered by any of the laminate combinations (aluminum stake on mild steel and vice versa).
- The experimental and theoretical strains exhibited their maximum values near the pole and then decreased gradually (in linear manner) toward the clamped edges.
- The strains in the aluminum sheets were much lower compared to that in mild steel sheets whether this was deformed as a single sheet or a part of a laminate. In the most cases, the longitudinal strains is much lower than the others strains.
- The fracture mode of mild steel sheet either in single or laminated diaphragm was almost near the pole area as short tear.
- The fracture mode of aluminum sheet as single diaphragm was similar to that in the mild steel. Whereas in laminated diaphragm was depended on the combination of laminate. When the mild steel stacked on the aluminum sheet, the fracture mode was by burst at the pole area.
- The rolling direction has no effect on the fraction location either for single diaphragm or laminated diaphragms.

REFERENCES

[1]   Lazarescu,L., Coma, D., Nicodim, I, Ciobanu,I and Banabic, " Characterization of plastic behavior of sheet metals by hydraulic bulge test", Trans. Nonferrous Met. Sco. China, Vol. 22, PP 275- 279, (2012).

[2]   Spisak, S.E., " Determination of flow stress by hydraulic bulge test", Metalurgua, Vol. 47, No 1, PP 13-14, (2008). Slovakia.

[3]   Gago, V., Feschiev, N., Comsa, D. and Minev, E.," Strain Hardening Evaluation by bulge testing of sheet metals", Proceeding to the 12th International Scientific Conference, Achievements in Mechanical & Materials Engineering, (2003).

[4]   Santos, A.D., Mendes, J.G., Alimeida, F.G., Teixeira, P., Mao,S. and Rocha, B., " Developing a bulge tester for sheet metal stress strain determination", Proceeding to the 3rd International Conference on Integrity, Reliability and Failure, Porto-Prtugal, 20-24 July, (2009).

[5]   Yousif, M.I, Duncan, J.L and Jounson, W, "Deformation and Failure of Thin Elliptical Diaphragms", International Journal Mech. Sci., Vol. 12, PP. 959-972, (1970).

[6]   Tomov, B., Gagov,V.,Yankov,E. and Radev,R., " Research highlights of sheet metal testing by hydraulic bulging" , Journal of Achievements in Materials and Manufacturing Engineering, Vol. 48, No 1, May (2011).

[7]   Kim, J, Hoffmann, H., Golle, R." Determination of Uniaxial flow stress Curve Using Aero- Bulge Test for Very thin Copper sheet", Advanced Materials Research, Vols. 264-265, PP 608-613, (2011).

[8]   Sobotka, J., Solfronk, P., Doubek, P. and Zuzanek, L., "The Hydrolic Test and its Importance for the Vegter Yield Criterion", Proceeding to Conference (METAL 2013), 15-17, May, 2003, Brno, Czech, Republic, EU.

[9]   Lu T., Chen C., Zhao k., Zhang W. and Wang T.J., " Bulge test at nano-scale: Surface effect", Appl. Phys. Lett, Vol. 103, 053110 (2013).

[10]   Janbakhsh, M., Djavanroodi, F. and Riahi, M., "Utilization of bulge and uniaxial tensile tests for determination of flow stress curves of selective ansitropic alloys", Proceeding of the Istitution of Mechanical Engineering, Part L: Journal of Materials: Design and Applications, Vol. 227, No. 4, First October (2013).

[11]   Soldatos,K.P," Refined Laminated plate and shell theory with application", Journal of Sound and Vibration, Vol.44, PP 786-790, (1991).

[12]   Gavrilenko,G.D," Calculation of the Stress-Strain State of Laminated Cylinder Shells" , Strength of Materials, Vol. 20, PP 786-790, (1989).

[13]   Patlashenko,I.YU.," Some Variants of the Approximate Theories of Laminated Plate Calculation", Soviet Applied Mech., Vol. 23, PP 667-673 , (1987).

[14]   ASME Boiler and Pressure Vessel, Section II, Material Specification, Parts A and B: Ferrous and nonferrous, 1972 edition.

[15]   Ducan,J.L. and Johnson,W.," The Ultimate Strength of Rectangular Diaphragms", Int. J. Mech. Sci. , Vol. 9, PP 681-696, (1967).

[16]   Gutscher,G., Chin Wu, H., Ngaile, G. and Altan, T., " Determination of flow stress for sheet metal forming using the viscous pressure bulge (VPB) test", J. of Mate. Proc. Techn., Vol. 146, PP 1-7, (2004).

NOMENCLATURES

σ_{yp} Yield stress

σ_{ult} Ultimate stress

ε_{yp} Yield strain

ε_{ult} Ultimate strain

E   Modulus of elasticity

ε_x Longitudinal strain along the minor axis

ε_y Transverse strain along the major axis

ε_t Thickness strain

(x_{i+1}) Incremental displacement in the minor axis

(x_i) Initial displacement in the minor axis

(y_i) initial displacement in the major axis

(t_o) initial thickness

(t_i) final thickness

(t_s) Thickness of mild steel sheet

(t_a) thickness of aluminum sheet

a , b   Minor and major die dimensions

P   hydrostatic pressure

h   central height of the diaphragm

ρ_x radius of curvature of minor axis

ρ_y Radius of curvature of major axis

σ_{xeq} equivalent stress of laminated sheet in minor axis

σ_{yeq} equivalent stress of laminated sheet in major axis

σ_{xs} stress of mild steel in minor axis direction

σ_{xa} stress of aluminum in minor axis direction

σ_{ys} stress of mild steel in major axis direction

σ_{ya} stress of aluminum in major axis direction